Electronic Supplementary Material (ESI) for Journal of Materials Chemistry A.


# A Fe-N-C hybrid electrocatalyst derived from bimetal-organic framework for efficient oxygen reduction

Teng Liu, Pingping Zhao, Xing Hua, Wei Luo,* Shengli Chen* and Gongzhen Cheng

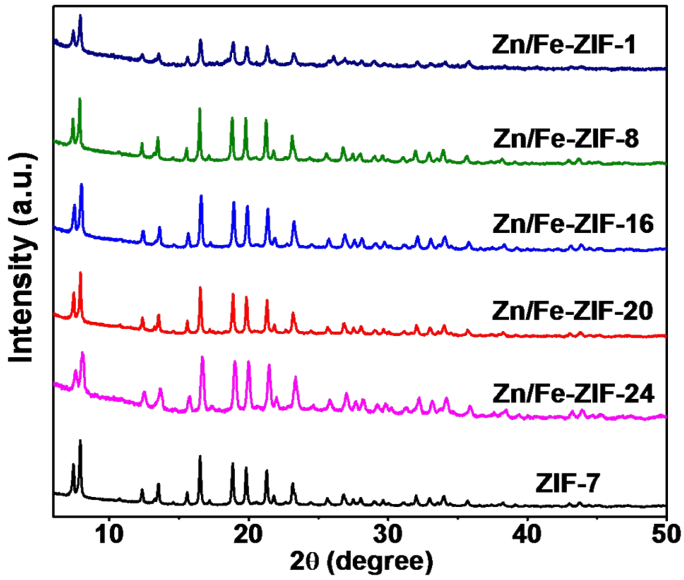


**Figure S1.** XRD survey of the Zn/Fe-ZIF-X.


**Figure S2.** Photographs of (a) ZIF-7, (b) Zn/Fe-ZIF-24, (c) Zn/Fe-ZIF-20, (d) Zn/Fe-ZIF-16, (e) Zn/Fe-ZIF-8 and (f) Zn/Fe-ZIF-1.

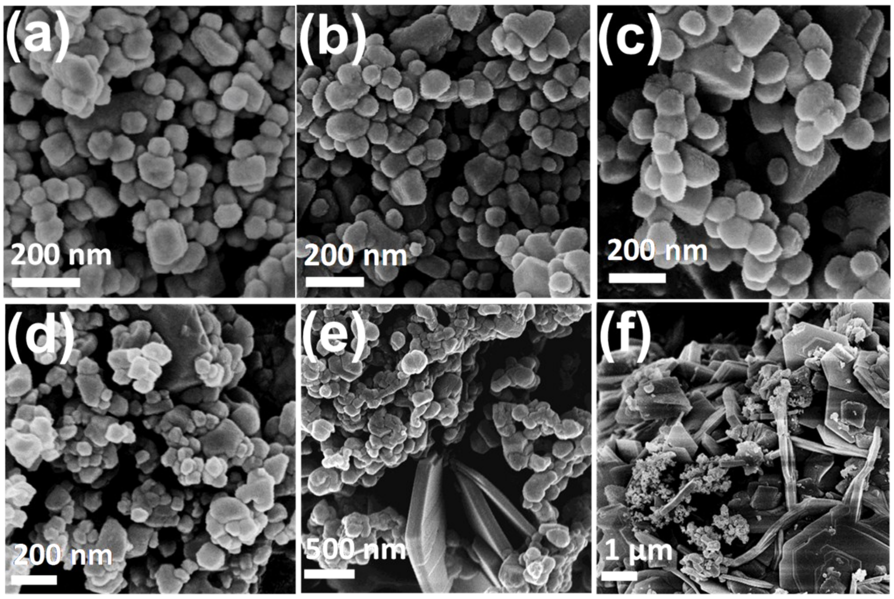


**Figure S3.** SEM images of (a) ZIF-7, (b) Zn/Fe-ZIF-24, (c) Zn/Fe-ZIF-20, (d) Zn/Fe-ZIF-16, (e) Zn/Fe-ZIF-8 and (f) Zn/Fe-ZIF-1.

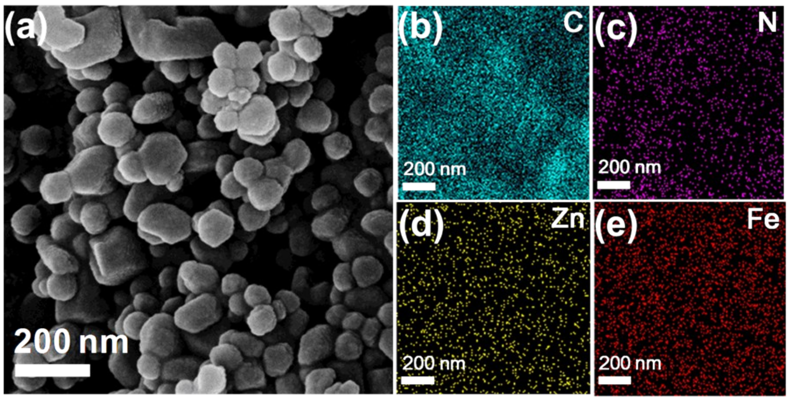


**Figure S4.** (a) SEM image of Zn/Fe-ZIF-20, (b-e) the elemental distribution of C,N, Zn and Fe.

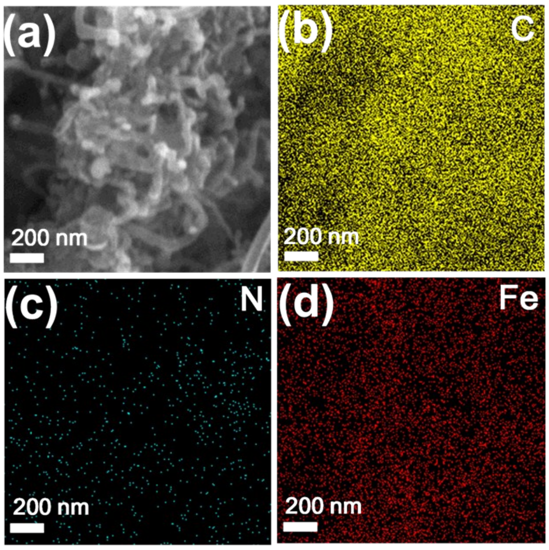


**Figure S5.** (a) SEM image of FeNC-20-1000, (b-d) the elemental distribution of C, N and Fe.

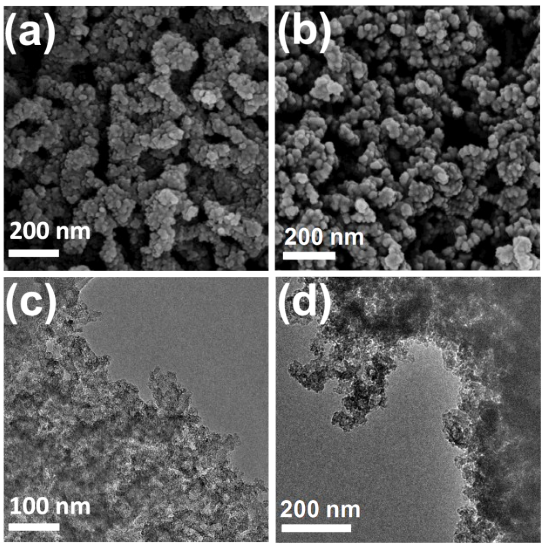


**Figure S6.** SEM image of (a) FeNC-20-900, (b) FeNC-20-1100. TEM image of (c) FeNC-20-900, (d) FeNC-20-1100.

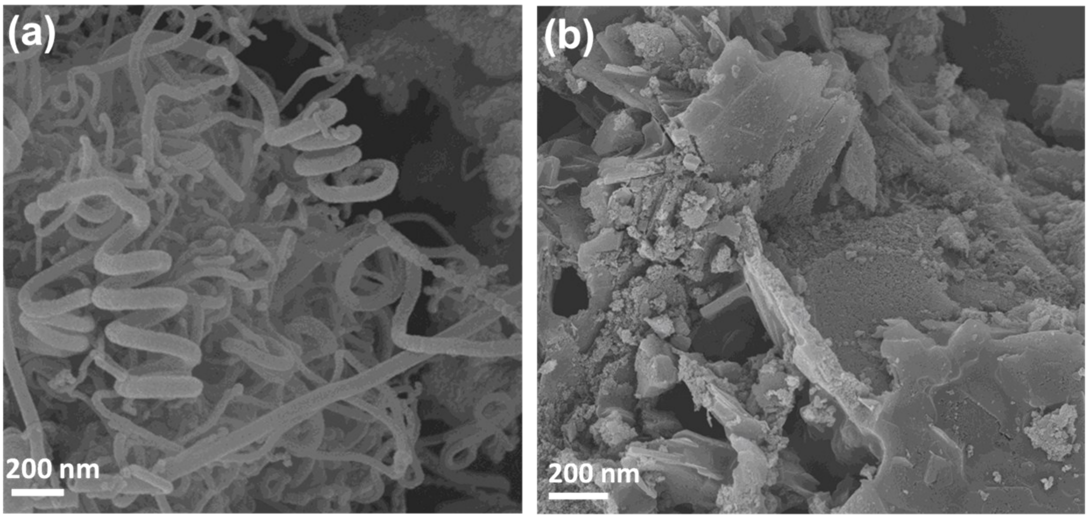


**Figure S7.** SEM images of (a) FeNC-20-1000-0, (b) FeNC-20-1000-con.

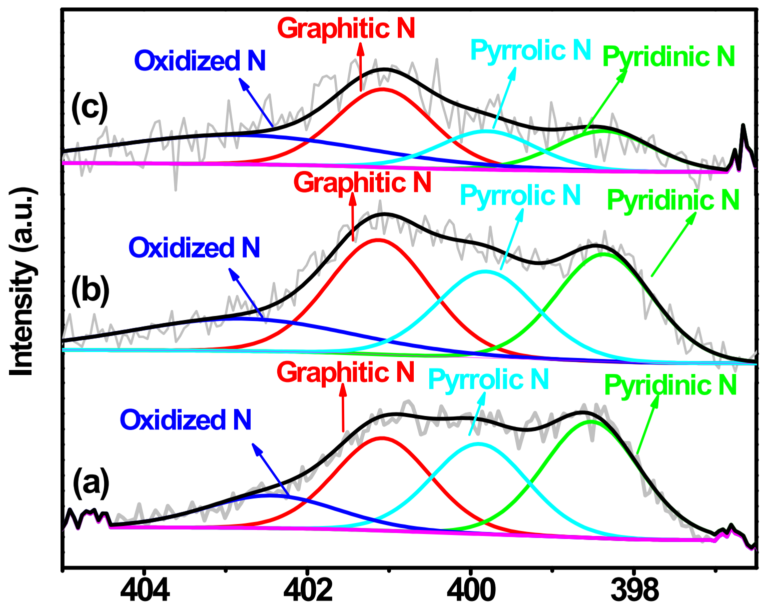


**Figure S8.** N 1s spectrum of FeNC-20-900 (a), FeNC-20-1000 (b), FeNC-20-1100 (c).

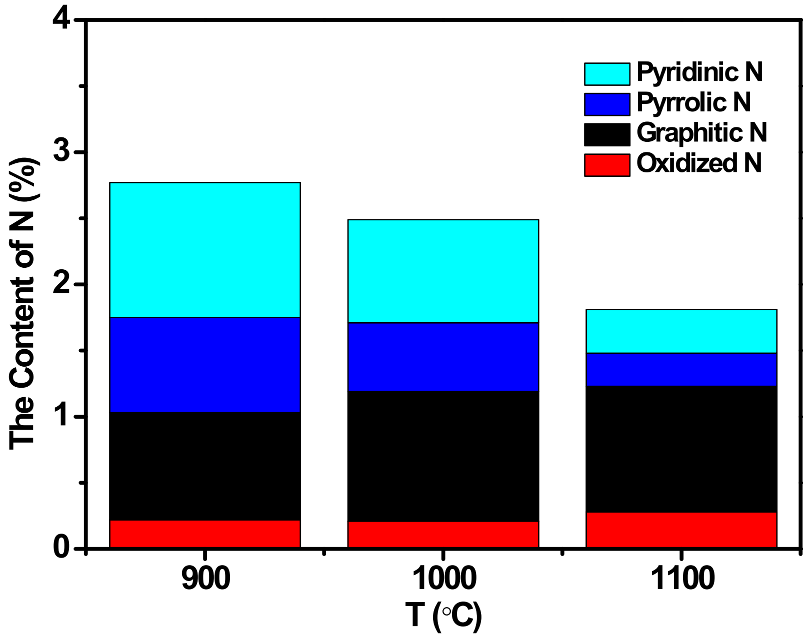


**Figure S9.** The content of N at different temperatures of 900, 1000 and 1100 °C respectively.

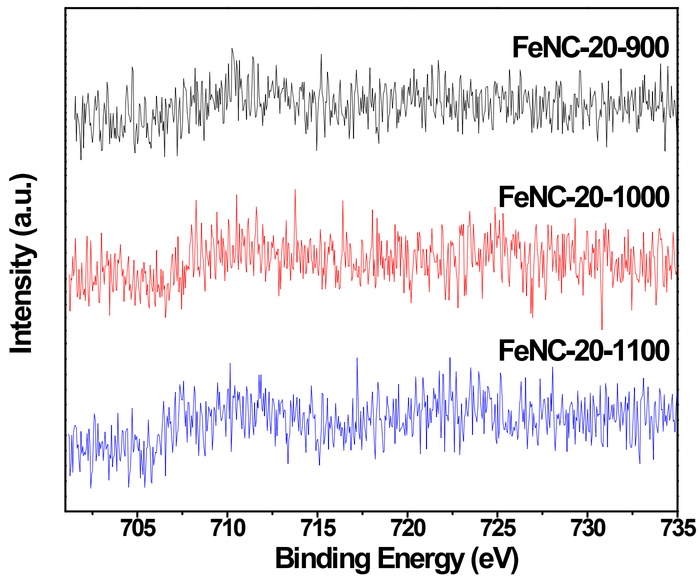


**Figure S10.** Fe 2p spectrum of FeNC-20-900, FeNC-20-1000, FeNC-20-1100.

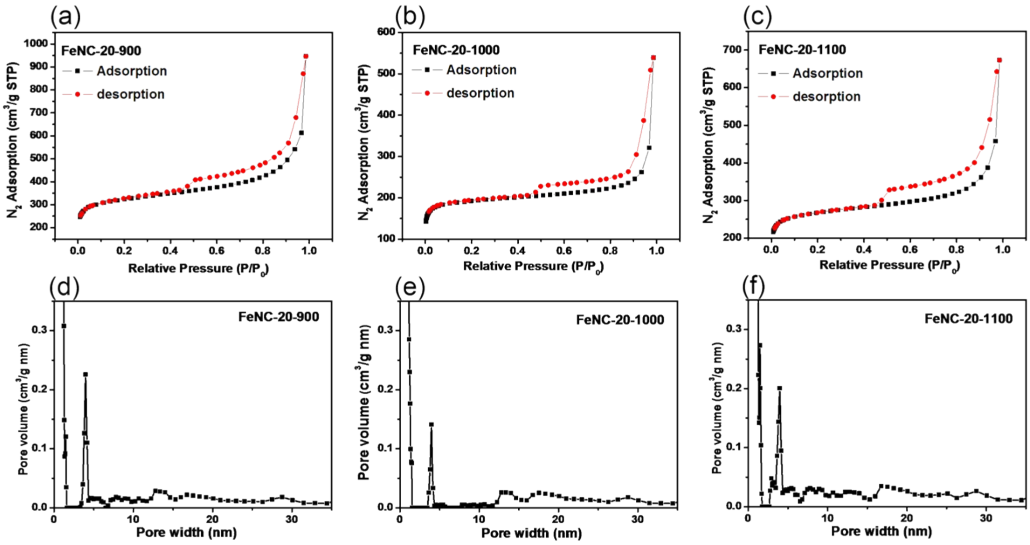


**Figure S11.** Nitrogen adsorption/desorption isotherms and pore distribution of FeNC-20-900, FeNC-20-1000, FeNC-20-1100.

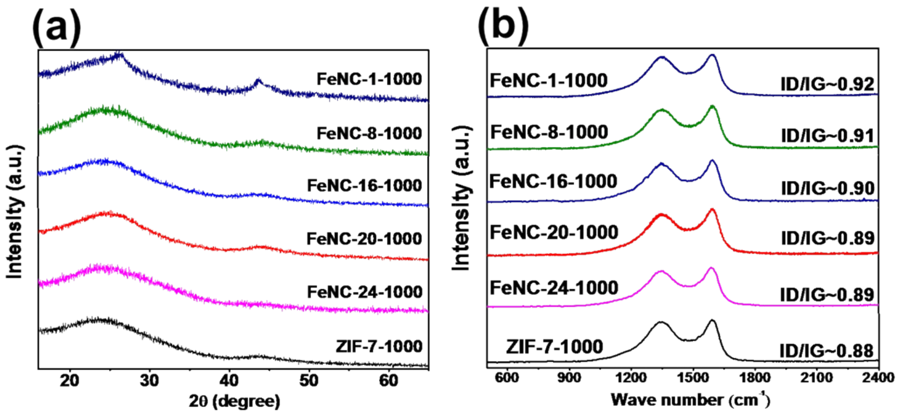


**Figure S12.** XRD pattern (a) and Raman spectra (b) of FeNC-X-1000.

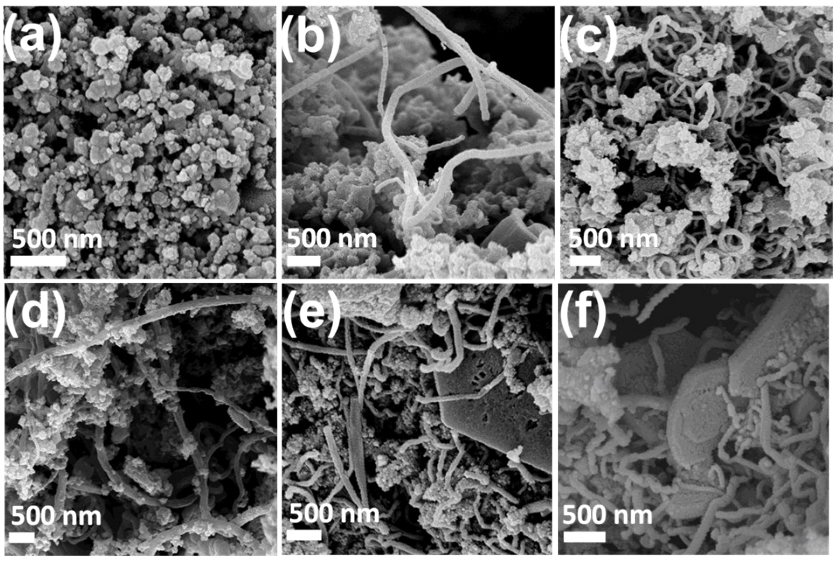


**Figure S13.** SEM image of (a) ZIF-7-1000, (b) FeNC-24-1000, (c) FeNC-20-1000, (d) FeNC-16-1000, (e) FeNC-8-1000, (f) FeNC-1-1000.

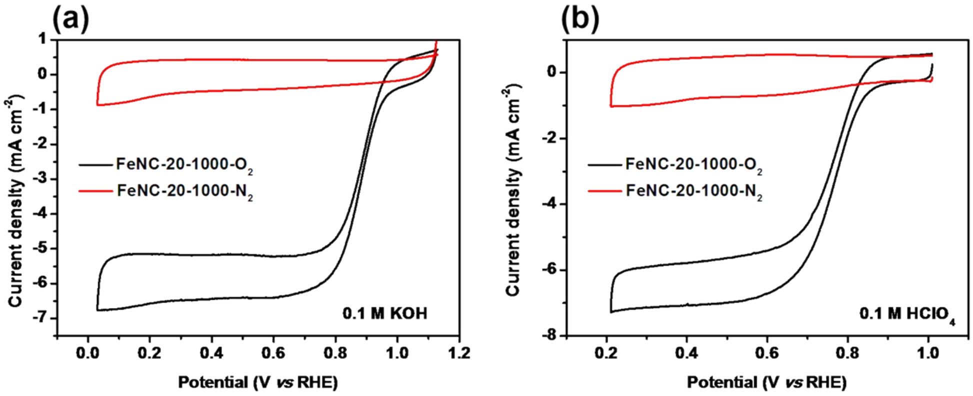


**Figure S14.** CV curve of FeNC-20-1000 in $N_2$ and $O_2$, the catalyst loading is 0.75 mg $cm^{-2}$.

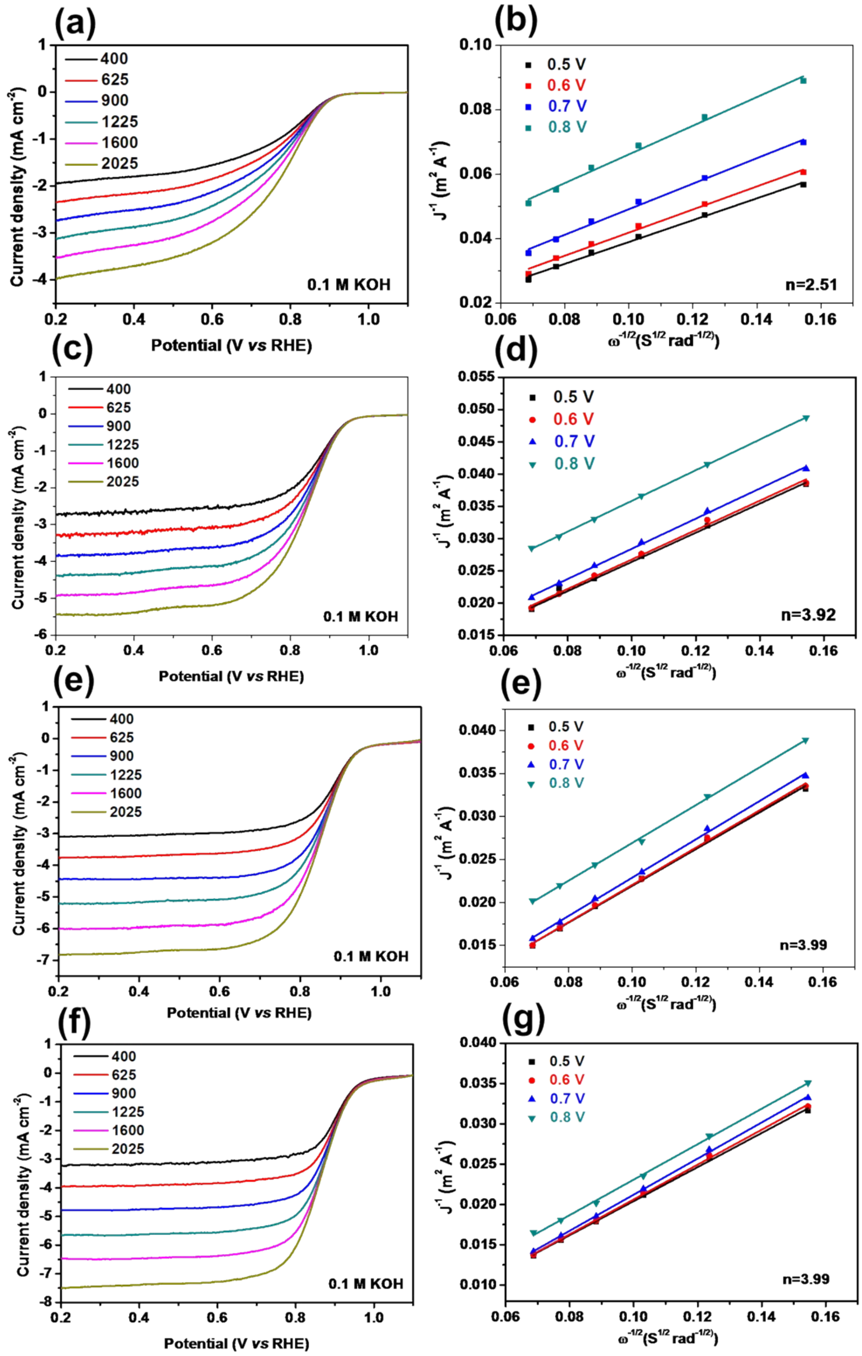


**Figure S15.** RDE voltammograms at different rotating speeds for FeNC-20-1000 with various catalyst loading and its corresponding Koutecky-Levich plots (a, b) 0.03 mg cm$^{-2}$, (c, d) 0.15 mg cm$^{-2}$, (e, f) 0.45 mg cm$^{-2}$ and (f, g) 0.75 mg cm$^{-2}$ in 0.1 M KOH with oxygen saturated.

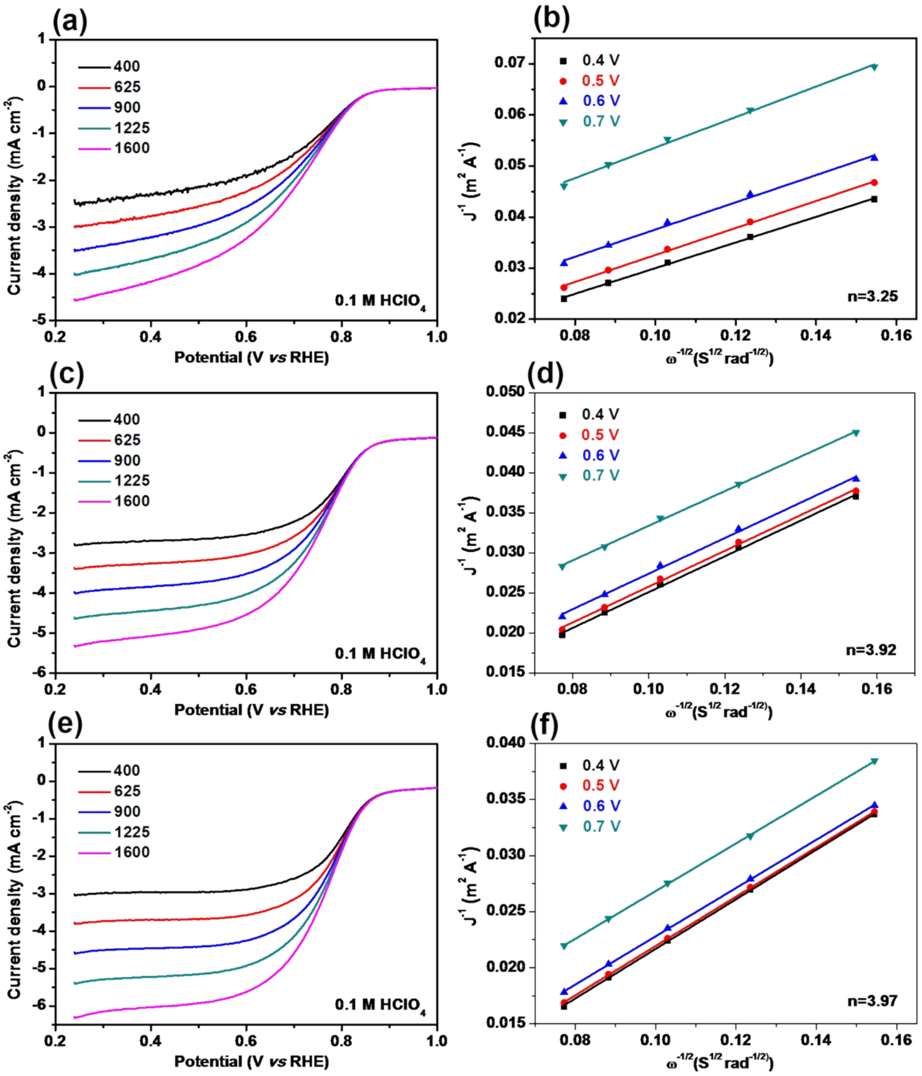


**Figure S16.** RDE voltammograms at different rotating speeds for FeNC-20-1000 with various catalyst loading and the corresponding Koutecky-Levich plots in 0.1 M $HClO_4$: (a, b) 0.15 mg $cm^{-2}$, (c, d) 0.45 mg $cm^{-2}$, (e, f) 0.75 mg $cm^{-2}$.

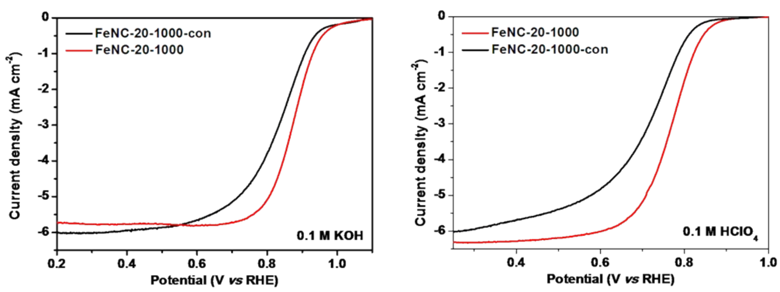


**Figure S17.** LSV curve of (a) FeNC-20-1000-con and (b) Pt/C carried in (a) 0.1 M KOH, (b) 0.1 M $HClO_4$ with oxygen saturated, rotating speed of 1600 rpm and a scan rate of 5 mV $s^{-1}$. Catalysts loading was 0.75 and 0.15 mg $cm^{-2}$ for FeNC-20-1000-con and Pt/C respectively.

**Table S1.** Comparison of the $E_{onset}$ and $E_{1/2}$ toward ORR for non-noble metal catalysts reported and this work in alkaline medium.

| **Catalyst** | **$E_{oneset}$/ V** | **$E_{1/2}$/V** | **Reference electrode** | **References** |
|---|---|---|---|---|
| Fe- N/C-800 | 0.923 | 0.809 | *vs* RHE | *J. Am. Chem. Soc.* **2014**, *136*, 11027 |
| $Fe_3C$/C-800 | 1.05 | 0.83 | *vs* RHE | *Angew. Chem. Int. Ed.* **2014**, *53*, 3675 |
| N-doped Fe/$Fe_3C$@C | 0.91 | 0.83 | *vs* RHE | *Adv. Energy Mater.* **2014**, *4*, 1400337 |
| PCN-FeCo/C | 1 | 0.85 | *vs* RHE | *Adv. Mater.* **2015**, *27*, 3431 |
| $Fe_3C$/C-800 | 1.03 | 0.86 | *vs* RHE | *Adv. Mater.* **2015**, *27*, 2521 |
| Fe-N-CNS | 0.98 | 0.85 | *vs* RHE | *ACS Catal.* **2015**, *5*, 3887 |
| Fe-N/C-800 | 0.98 | / | *vs* RHE | *J. Am. Chem. Soc.* **2015**, *137*, 5555 |
| $CoFe_2O_4$/NG | -0.03 | -0.144 | *vs* Ag/AgCl | *Small* **2015**, *11*, 5833 |
| Fe-N-CNFs | -0.02 | -0.14 | *vs* Ag/AgCl | *Angew. Chem. Int. Ed.* **2015**, *54*, 8179 |
| Co@$Co_3O_4$@C–CM | 0.93 | 0.81 | *vs* RHE | *Energy Environ. Sci.* **2015**, *8*, 568 |
| FePhen@MOF-$ArNH_3$ | 1.03 | 0.86 | *vs* RHE | *Nat. Commun.* **2015**, *6*, 7343 |

| | | | | |
|---|---|---|---|---|
| $Co_3O_4$@CMWCNT | 0.89 | 0.81 | *vs* RHE | *J. Mater. Chem. A* **2015**, *3*, 17392 |
| Co -S/G-3 | 0.93 | 0.83 | *vs* RHE | *ACS Appl. Mater. Interfaces* **2015**, *7*, 21373 |
| GNS/MC | / | 0.85 | *vs* RHE | *Adv. Energy Mater.* **2016**, 1501794 |
| pPMF-800 | 1.05 | 0.879 | *vs* RHE | *Nanoscale* **2016**, *8*, 959 |
| Fe/N/CNT | 1.04 | 0.86 | *vs* RHE | *Appl. Catal. B: Environ.* **2016**, *183*,185 |
| FeNC-20-1000 | 1.04 | 0.88 | *vs* RHE | This work |

**Table S2.** Comparison of the $E_{onset}$ and $E_{1/2}$ toward ORR for non-noble metal catalysts reported and this work in acid medium. The mole concentration in the table is 0.5 M for $H_2SO_4$ and 0.1 for $HClO_4$.

| Catalyst | $Ea_{oneset}$/V | $E_{1/2}$/V | Electrolyte | References |
|---|---|---|---|---|
| PANI-Fe-C | 0.93 | / | $H_2SO_4$ | *Science* **2011**, *332*, 443 |
| NT-G | 0.89 | 0.76 | $HClO_4$ | *Nat. Nanotech.* **2012**, *7*, 394 |
| PFeTTPP-1000 | 0.93 | 0.76 | $HClO_4$ | *Angew. Chem. Int. Ed.* **2013**, *125*, 8507 |
| Fe-AAPyr | 0.9 | 0.75 | $H_2SO_4$ | *Electrochimi. Acta* **2013**, *90*, 656 |
| PpPD-Fe-C | 0.826 | 0.718 | $H_2SO_4$ | *Angew. Chem. Int. Ed.* **2014**, *53*, 2433 |
| $Zn(eIm)_2$TPIP | 0.914 | 0.78 | $HClO_4$ | *Adv. Mater.* **2014**, *26*, 1093 |

| | | | | |
|---|---|---|---|---|
| $Fe_3C$/C-700 | 0.9 | 0.73 | $HClO_4$ | *Angew. Chem. Int. Ed.* **2014**, *53*, 3675 |
| Fe-N-GC-900 | / | 0.74 | $HClO_4$ | *ACS Catal.* **2014**, *4*, 1793 |
| PMF-800 | 0.886 | / | $HClO_4$ | *J. Am. Chem. Soc.* **2015**, *137*, 1436 |
| PCN-FeCo/C | 0.9 | 0.76 | $HClO_4$ | *Adv. Mater.* **2015**, *27*, 3431 |
| $Fe_3C$/NG-800 | 0.92 | 0.77 | $HClO_4$ | *Adv. Mater.* **2015**, *27*, 2521 |
| CPANIFe-NaCl | 0.91 | 0.74 | $HClO_4$ | *J. Am.Chem. Soc.* **2015**, *137*, 5414 |
| N–Fe/G (60)-900-S | 0.834 | 0.716 | $HClO_4$ | *Nanoscale* **2015**, *7*, 14707 |
| pPMF-800 | 0.89 | 0.71 | $HClO_4$ | *Nanoscale* **2016**, *8*, 959 |
| ZIF-TAA-p | 0.88 | 0.78 | $HClO_4$ | *J. Mater. Chem. A* **2016**, *4*, 4457 |
| FeNC-20-1000 | 0.90 | 0.77 | $HClO_4$ | This work |